

# Characterization of the Effect of the Inlet Operating Conditions on the Performance of Lean Premixed Gas Turbine Combustors

J.L. Samperio\*, J.G. Lee\*\* and D.A. Santavicca\*

## ABSTRACT

An experimental study of the effect of operating conditions on the behavior of a lean premixed laboratory combustor operating on natural gas has been conducted. Measurements were made characterizing the pressure fluctuations in the combustor and the flame structure over a range of inlet temperatures, inlet velocities and equivalence ratios. In addition the fuel distribution at the inlet to the combustor was varied such that it was an independent parameter in the experiment. Inlet temperature, inlet velocity and equivalence ratio were all found to have an effect on the stability characteristics of the combustor. The nature of this effect, however, depended on the fuel distribution. For example, with one fuel distribution the combustor would become unstable when the temperature was increased, whereas with a different fuel distribution the combustor would become unstable when the temperature was decreased. Similarly, the operating conditions had an effect on the flame structure. For example the intensity-weighted center of mass of the flame was found to move closer to the center body as either the temperature or equivalence ratio increased. It was interesting and somewhat surprising to note, however, that as the location of the center of mass changed with operating conditions it did so by moving along a line of constant flame angle.

**Key Words:** Combustion dynamics, Turbulent flame structure, Gas turbine combustor

## Nomenclature

CB	Centerbody injection	$U_m$	Velocity in mixing section
DS	Downstream injection	$U_c$	Velocity in combustor
PM	Premixed injection	$\phi$	Equivalence ratio
$T_i$	Inlet mixture temperature		

## 1. INTRODUCTION

Oscillating combustion in lean premixed gas turbine (LPGT) combustors is known to occur when variations in heat release are coupled with the acoustic characteristics of the system. Following Rayleigh's criterion the oscillations will be amplified if changes in heat release are in phase with the acoustic disturbances. In addition to Rayleigh's criterion a closed feedback loop

between the heat release fluctuations, its driving mechanism and the acoustic oscillations is necessary to maintain the instability. Several processes have been proposed as the driving mechanism for such periodic heat release fluctuations. Flame-vortex interactions [1-3] and feed system coupling [4-6] are generally considered to be the most important of these mechanisms.

Flame-vortex interaction refers to the interaction between the flame front and vortices which are periodically shed at the entrance to the combustor. As the vortex passes through the flame front, the flame is wrapped around the vortex, increasing its length and as a result the overall heat release.

\* Department of Mechanical & Nuclear Engineering,  
The Pennsylvania State University, University Park,  
PA 16802

† 연락처자, jxl145@psu.edu

Feed system coupling refers to a modulation of the air and/or fuel flow which is caused by the pressure fluctuations. This results in equivalence ratio fluctuations which convect from the injector to the combustor. If the equivalence ratio fluctuation arrives at the flame front in-phase with the heat release fluctuation it drives the instability, while, if it arrives out-of-phase with the heat release fluctuation it damps the instability.

In order to develop an improved understanding of combustion dynamics it is essential to have an understanding of the relative importance of the instability driving mechanisms and how that changes with operating conditions. A number of studies [3-4,6-13] have shown that the stability characteristics of lean premixed combustors change significantly with operating condition, i.e., with equivalence ratio, inlet velocity, inlet temperature and inlet fuel distribution. However, it has also been shown that the dependence on operating condition is not universal, i.e., it varies with the combustor design. The work presented in this paper represents preliminary results from a study of the effect of operating conditions on combustion dynamics through changes in the relative importance of the instability driving mechanisms. It is expected that results from this study will lead to an understanding of the effect of combustion system geometry on the relationship between combustion dynamics and combustor operating conditions.

## 2. Experimental apparatus and procedure

### 2.1 Apparatus

The facility where the experiments were conducted is comprised of four main systems: combustion air supply system, cooling air system, fuel delivery system, and combustor as illustrated in Fig. 1.

The combustion air is supplied by a high pressure compressor and is preheated using a 35 kW electric heater. The combustion air is choked at the inlet to the combustor.

Cooling air is directed onto the fused-silica walls of the optically-accessible combustion chamber through twenty 1.6 mm diameter holes. The holes are equally spaced around the circumference of a cooling ring located outside the fused-silica

section and flush with the dump plane. This air supply to the cooling ring is independent of the combustion air supply system.

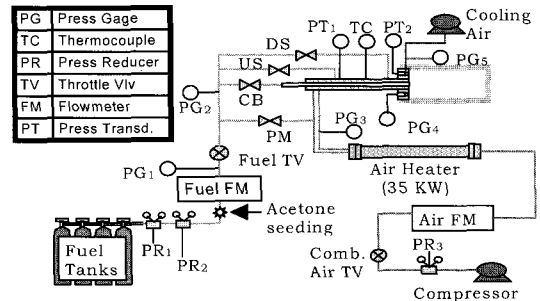
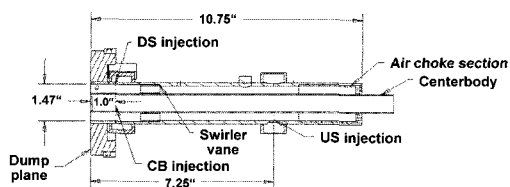


Fig. 1 Flow diagram

Natural gas (94% methane) was the fuel used in the experiments. The fuel pressure is set at 200 psig. The total fuel flow rate is monitored using a mass flowmeter, downstream of which the fuel line splits into four different lines for each of the injection locations. Each fuel injection line is provided with a flowmeter to allow for accurate fuel splits between any of the injection locations.

The combustor is an optically accessible co-axial dump combustor with a bluff centerbody and a radial swirler. The 19 mm diameter centerbody is positioned coaxially inside the 37 mm diameter mixing section and flush mounted with the dump plane. The 30° axial swirler is mounted in the mixing section 51 mm upstream of the dump plane. The inlet to the mixing section is choked. The combustion chamber (815 mm long) consists of an optically accessible, fused-silica section (110 mm ID and 230 mm long) followed by a (78 mm ID and 585 mm long) stainless-steel section. At the end of the stainless-steel section there is a 19 mm dia(OD) restriction, which although not choked provides a reflective acoustic boundary.

The apparatus is provisioned with 4 different fuel injection locations, three of them are used to produce partially-premixed fuel distributions (Fig. 2), and the fourth one produces a 100% premixed fuel distribution. One of the partially-premixed injection locations is referred to as centerbody (CB) injection. In this case the fuel is injected radially outward through the centerbody into the mixing section through 16 equally spaced holes (0.635 mm diameter) located 25.4 mm upstream of



**Fig. 2 Schematic drawing of the mixing section**

the dump plane. The other two partially-premixed injection locations are referred to as downstream (DS) injection and upstream (US) injection. In both cases the fuel is injected radially inward through the outer wall of the mixing section through 12 (0.406 mm dia) holes. The downstream injection location is 25.4 mm upstream of the dump plane (and therefore directly opposite the CB injection holes). The upstream injection location is 185 mm upstream of the dump plane. The fourth injection location is well upstream of the choked inlet to the mixing section and produces a uniform fuel distribution. This is referred to as 100% premixed (100% PM) injection.

The inlet air temperature is monitored using a k-type thermocouple located 82 mm upstream of the dump plane. The velocity and equivalence ratio values were obtained from the air and fuel flowmeters. The combustor oscillations are measured using a piezoelectric pressure transducer located flushed with the dump plane. The frequency spectrum was obtained from a frequency signal analyzer. Exhaust gas samples extracted 20 mm downstream of the combustor exit were analyzed using a chemiluminescence NO<sub>x</sub> analyzer.

## 2.2 Diagnostic techniques

To determine the radial and circumferential fuel distribution profiles for the four different injection locations, acetone PLIF [14] was used where the fuel is seeded with acetone. Since these measurements were made without combustion, the fuel was replaced with air whose amount is set in such a way that its momentum is matched with that of methane. The inlet air temperature for these measurements was set to 100 °C to avoid possible condensation of the acetone. The 4<sup>th</sup> harmonic (266 nm) of Nd:YAG laser was used as

the excitation source for the PLIF measurements. The output of the laser was formed into a 0.5 mm thick by 30 mm wide laser sheet which was positioned parallel to and approximately 1 mm downstream of the dump plane. An intensified CCD camera located downstream of the dump plane was used to capture the acetone fluorescence images and averages of 40 images were acquired per condition. Both background noise subtraction and a uniform field correction were applied to each of the 40-image averages.

CO<sub>2</sub> chemiluminescence imaging was used to characterize the flame structure[3,6,13]. Since this is inherently a line-of-sight measurement a deconvolution procedure was used to obtain two-dimensional images in order to reveal the flame structure[15]. The camera gate was set to 25 μsec for these measurements and a 40-images was acquired at each condition. In the case of an unstable flame, the camera was phase-synchronized with the pressure oscillation in order to obtain a sequence of 12 phase-synchronized images (in 30 degree increments) during one period of the instability. In addition to making qualitative comparisons of the flame structure at different operating conditions and intensity-weighted "center-of-mass" was calculated for each image to quantify changes in the flame structure with operating condition.

## 2.3 Test conditions

Tests were conducted over the range of operating conditions listed in Table 1. As discussed previously by splitting the fuel between the four different fuel injection locations it was possible to systematically vary the fuel distribution as part of the test matrix. As indicated in Table 1, four different fuel distributions were tested, i.e., corresponding to 100% centerbody (CB), 100% downstream (DS) injection, 100% premixed (100% PM) injection and 50%CB/50%DS injection. The fuel distributions achieved with each of the injection locations are presented in the results and discussion section.

The combustor inlet temperature was varied from 100 to 350 °C in increments of 50 °C. Tests were run at four combustor velocities, i.e., 3, 4.5, 6 and 7.5 m/s. These velocities refer to the one-dimensional velocity in the combustor at the inlet air temperature. The corresponding velocities

**Table 1. Operating conditions**

Injection Location	100% PM, CB, D/S and 50% CB / 50% DS split
Swirl Angle	30°
Combustor inlet temp.	100, 150, 200, 250 and 350° C
Combustor mean velocity	3-10 m/sec
Equivalence ratio	LBO to 0.775
Mean combustor pressure	0.07 to 0.35 bar

in the mixing section are a factor of twelve greater, i.e., 36, 54, 72 and 90 m/s. The equivalence ratio was varied from the lean blow out limit to 0.775 in increments of 0.025. All tests were conducted by increasing the equivalence ratio to avoid inconsistencies due to hysteresis effects.

All tests were conducted at a nominal combustor pressure of 1 atmosphere, however, at the highest flow rates the pressure in the combustor was as high as 1.5 atmospheres due to the restricted combustor exit.

### 3. Result and discussion

#### 3.1 Fuel distribution measurements

The fuel distribution at the exit of the annular mixing section was measured using acetone PLIF as described previously. The fuel distribution measurements were all made at an equivalence ratio of 0.700 and an inlet temperature of 100°C. Measurements were made at combustor velocities of 3, 4.5, 6 and 9 m/s.

The fuel distribution results for all four injection locations at a combustor velocity of 4.5 m/s are shown in Fig. 3. At the bottom of the figure the two-dimensional fuel distributions over the annular mixing section are shown in false-color. The color scale shows the relationship between color and equivalence ratio. The two-dimensional distributions shown in this figure are averages over 40 single-shot PLIF measurements. The PM case and the 50% CB/50%DS case both show relatively uniform fuel distributions, while the CB case shows that the equivalence ratio is greater near the outer wall of the mixing section, and the DS case shows that the equivalence ratio is greater along the centerbody. This is more clearly shown in the plots of equivalence ratio versus

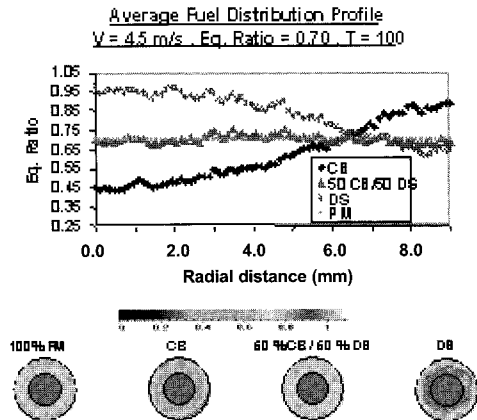


**Fig. 3 Fuel distribution across the annular mixing section**

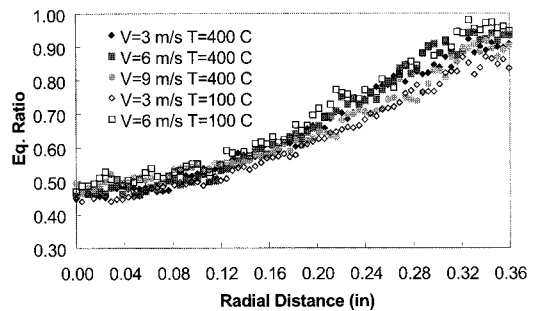


**Fig. 4 Effect of inlet velocity and temperature on fuel distribution**

radial distance that are shown above the two-dimensional fuel distributions. These profiles are averages of twelve radial profiles measured in increments of 30° around the annular mixing section. In other words, these are effectively circumferential averages.

Plots in Fig. 4 show the circumferential average fuel distribution profile at different temperatures (100 and 400°C) and velocities (3 to 9 m/s) for CB fuel injection. Variations in the equivalence ratio at any given radial location are within 5% of each other regardless of the temperature or the velocity. These results indicate that the fuel distribution profile can be effectively treated as an independent variable, so that any difference in the behavior of the combustor for two different injection locations at the same inlet operating conditions can be effectively attributed to the spatial distribution of the fuel/air mixture.

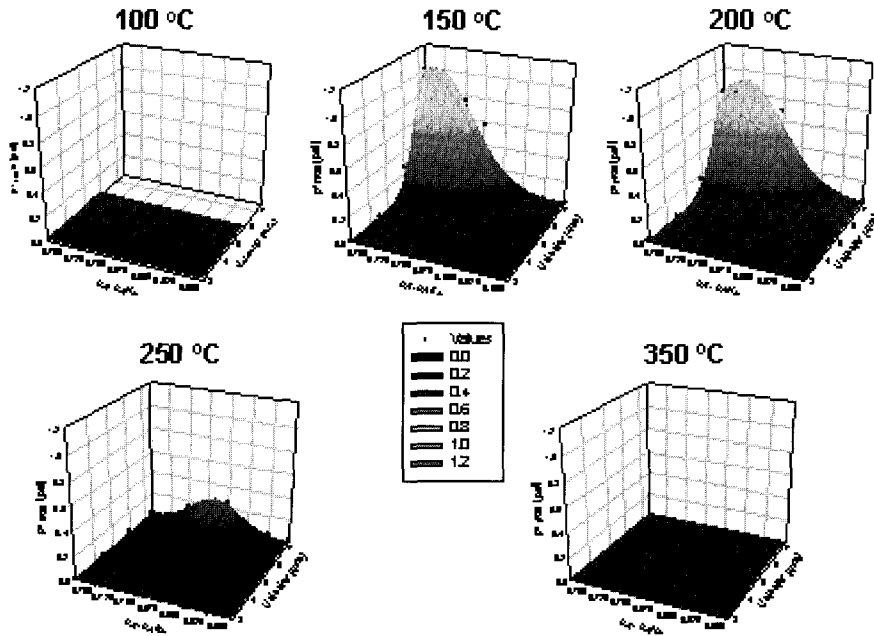


Fig. 5 Stability map for 100% premixed case

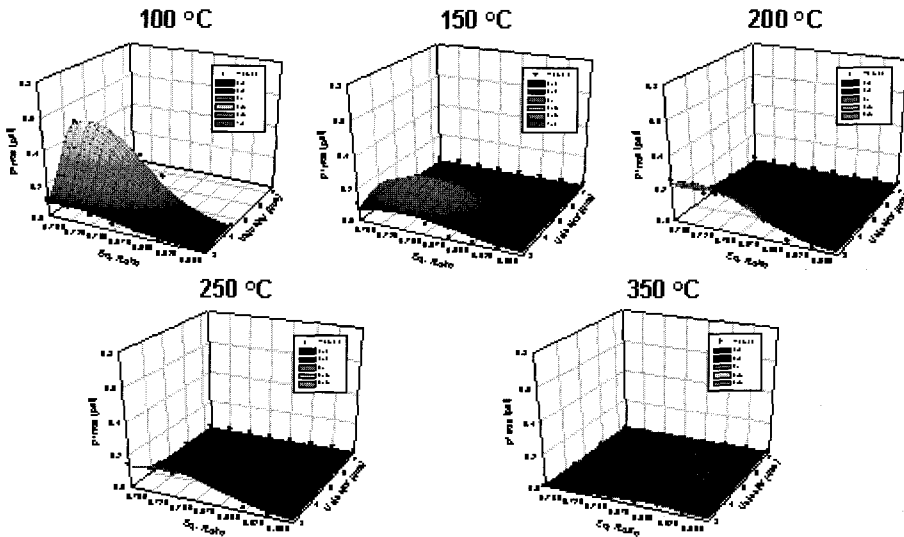


Fig. 6 Stability map for 100% centerbody case

### 3.2 Stability Map

The rms amplitude of the pressure oscillations for 32 combinations of velocity and equivalence (4 velocities and 8 equivalence ratios) were plotted at five different temperatures for each of the four fuel

distributions. The results for all four fuel distributions show that temperature, equivalence ratio and velocity have an effect on the stability of the combustor, but more importantly the results also show that the effect of these parameters is different for different fuel distributions.

This is illustrated in Fig. 5 and 6 where the

results for 100% premixed (100% PM) injection and for centerbody (CB) injection, respectively, are presented. As shown the data has been curve fit to 3-D surface plots in order to more clearly show trends in the results.

The results for 100% PM injection show that at the lowest (100°C) and highest (350°C) temperatures the combustor is stable over the entire range of velocities and equivalence ratios tested. (Note that at 100°C the flame blows out at the highest velocity condition, hence the absence of data at 7.5 m/s.) When the temperature is lowered to 250°C, instabilities begin to occur at the highest velocity (7 m/s) condition near the middle of the equivalence ratio range (~0.70), however, the maximum rms pressure fluctuation is only 0.2 psi. As the temperature is further decreased to 200°C, the strength of the instabilities at high velocity grow reaching a maximum rms pressure fluctuation of ~0.9 psi. The peak in the rms pressure fluctuation although still at the highest velocity has shifted to a higher equivalence ratio (~0.75). And finally, when the temperature is decreased to 150°C the strongest instability is observed ( $p_{rms}$  ~ 1.0 psi), where again the peak has shifted to even higher equivalence ratio (~0.775).

The results for CB injection presented in Fig. 6 show significantly different behavior than that of the 100% PM case just discussed. With CB injection the strongest instabilities are observed at the lowest temperature (100°C) condition, whereas no instabilities are observed at this temperature in the 100% PM case. Both injection cases, however, do show that the flame blows out at higher velocities, i.e., at ~7.5 m/s in the 100% PM case and at ~4.5 m/s in the CB injection case. Given the reduced equivalence ratio on the centerbody in the CB injection case this result is to be expected. Both injection cases also show that the strongest instabilities occur at the highest equivalence ratios.

As the temperature is increased from 100°C to 150°C in the CB injection case, the instability weakens and the peak in the stability map begins to shift to lower velocities. When the temperature is increased to 200°C the peak in the instability map has continued to shift to lower velocities, although the peak pressure fluctuation appears to have increased somewhat. As the temperature is increased to 250°C the instabilities are still observed at the lowest velocity condition,

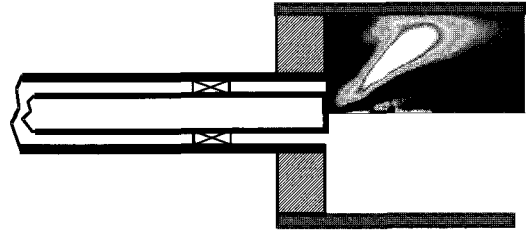


**Fig. 7 Location of flame structure images**

however, they have become noticeably weaker and the peak appears to be shifting to lower equivalence ratios. Finally at 350°C there is only evidence of a very weak instability ( $p_{rms}$  ~ 0.05 psi) at 3 m/s and at equivalence ratios near 0.65.

### 3.3 Flame structure measurements

The location of the flame structure images which are presented in this section is illustrated in Fig. 7. The effect of fuel distribution on flame structure is shown in Fig. 8 where flame structure images for a fixed velocity of 4.5 m/s, a fixed equivalence ratio of 0.7 and a fixed temperature of 250°C are presented. Note that the flame is stable at these conditions for all four fuel distributions. In the 100% PM case the flame is anchored on the centerbody and extends out all the way to the wall of the combustor. The flame structure in the 50%CB/50%DS case is very similar to the 100% PM case, which is reasonable since both have the same fuel distribution. The main difference between these two cases is that the 50%CB/50%DS case can experience feed system coupling, while the 100% PM case can not (because the fuel and air are mixed upstream of the choked inlet to the mixing section).

When all of the fuel is injected through the centerbody (CB) injection location, there is a noticeable shift in the location of the flame towards the outer wall of the combustor. This is consistent with the fact that with centerbody injection the fuel concentration is greatest away from the centerbody. Likewise, when all of the fuel is injected through the downstream injection location, the most intense region of the flame is shifted closer to the centerbody, which in this case is where the fuel concentration is greatest. It is interesting to note that although the location where the fuel burns changes as the fuel distribution changes, it appears to move along a line of fixed

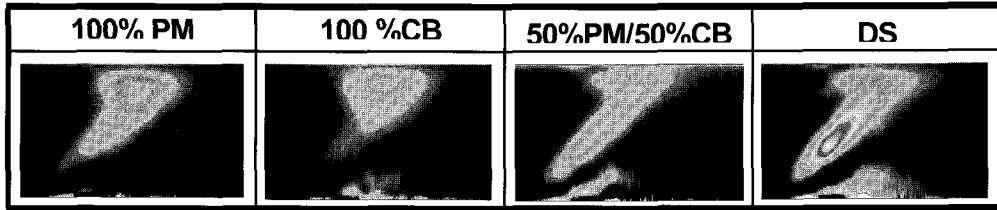


Fig. 8 Effect of Fuel Distribution on Flame Structure  $V_m=4.5\text{m/s}$ ,  $\phi=0.700$ ,  $T_i=250^\circ\text{C}$

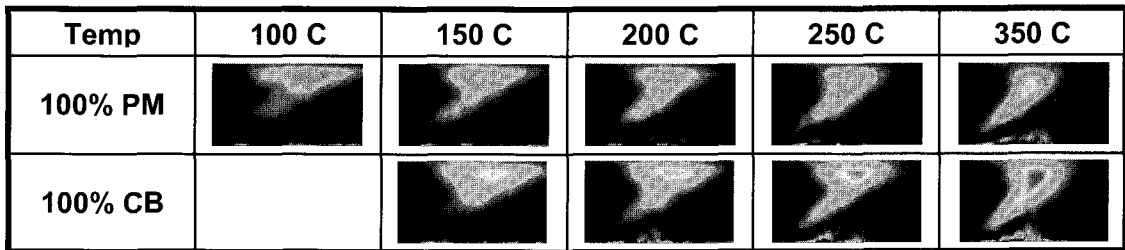


Fig. 9 Effect of Temperature on Flame Structure

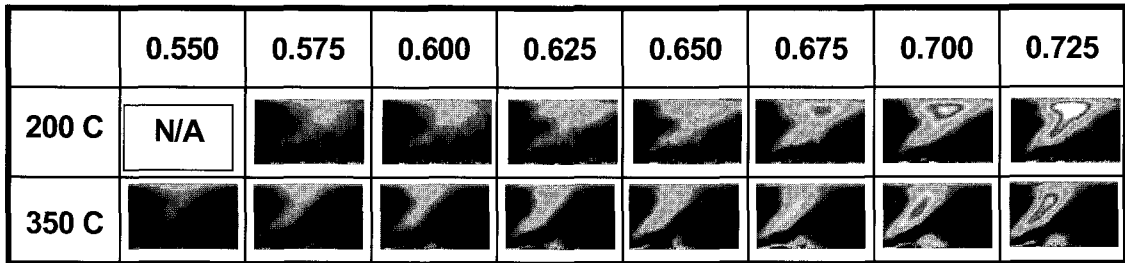


Fig 10. Effect of Equivalence Ratio on Flame Structure (100% PM,  $U_m=4.5\text{ m/s}$ )

flame angle.

The effect of temperature on flame structure is shown in Fig. 9 where flame structure images for the 100% PM case and the CB case at temperatures of  $100^\circ\text{C}$ ,  $150^\circ\text{C}$ ,  $200^\circ\text{C}$ ,  $250^\circ\text{C}$  and  $350^\circ\text{C}$  are presented. Again the flame is stable at all conditions shown. In the 100% PM case, as the temperature increases there is a small increase in the flame angle (relative to the axis of the combustor), and the region of most intense combustion spreads out towards the centerbody. The same behavior is observed in the CB flame images where again there is a small increase in flame angle with increasing temperature as well as a spreading of the region of combustion towards from the centerbody. This behavior is consistent with the fact that the flame blows out as the

temperature is decreased, as it does in the CB case at  $100^\circ\text{C}$ .

The effect of equivalence ratio on flame structure is shown in Fig. 10, where flame structure images for 100% PM injection at temperatures of  $200^\circ\text{C}$  and  $350^\circ\text{C}$  over a range of equivalence ratios from 0.550 to 0.725. Again the flame is stable at all conditions shown. The effect of equivalence ratio on the flame structure is very similar to that of temperature in that there is a small increase in flame angle as the equivalence ratio is increased (as the temperature is increased) and the region of combustion spreads out closer to the centerbody. The fact that temperature and equivalence ratio have the same effect on flame structure indicates that this effect is the result of changes in the flame speed.

### 3.3 Center of Mass

In order to quantify the effect of the different operating conditions on flame structure, the location of the intensity-weighted center of mass (COM) of each stable image was calculated. It can be argued that the bulk of the combustion process occurs in the vicinity of the center of mass, therefore its behavior as the conditions change make it a good indicator of the overall flame response.

Figure 11 is a graph showing the location of the COM for all of the 100% PM and all of the CB stable operating conditions. It is observed that as the operating conditions are varied, the COM moves along a line with an angle of approximately  $32^\circ$  relative to the axis of the combustor. This is consistent with the previous observation that the flame angle only appeared to change a small amount as the operating conditions were changed.

The distance of the COM from the edge of the centerbody was also calculated and a correlation was derived expressing the distance to the center of mass as a function of the temperature, velocity and equivalence ratio. Although not discernable from this figure, the data shows that the COM moves closer to the centerbody as either the temperature or equivalence ratio are increased, while it moves away from the centerbody as the velocity is increased. The correlation also indicates that changes in the equivalence ratio and temperature have a much larger effect on the location of the COM than changes in the velocity. A comparison of the 100% PM and CB correlations indicates that the effect of equivalence ratio on the location of the COM was significantly greater in the 100% PM case than in the CB case.

## 4. Conclusions

An experimental study of the effect of operating conditions on the behavior of a lean premixed laboratory combustor operating on natural gas has been conducted. Measurements were made characterizing the pressure fluctuations in the combustor and the flame structure over a range of inlet temperatures, inlet velocities and equivalence ratios. In addition the fuel distribution at the inlet to the combustor was varied such that it was an independent parameter in the experiment.

Inlet temperature, inlet velocity and equivalence

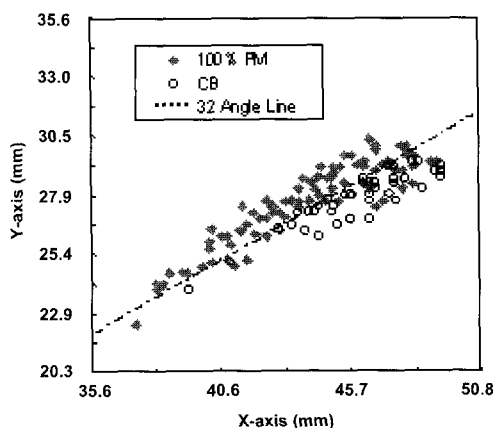


Fig.11 Location of center of mass

ratio were all found to have an effect on the stability characteristics of the combustor. The nature of this effect, however, depended on the fuel distribution. For example, with one fuel distribution the combustor would become unstable when the temperature was increased, whereas with a different fuel distribution the combustor would become unstable when the temperature was decreased.

Similarly, the operating conditions had an effect on the flame structure. For example the intensity-weighted center of mass of the flame was found to move closer to the center body as either the temperature or equivalence ratio increased. It was interesting and somewhat surprising to note, however, that as the location of the center of mass changed with operating conditions it did so by moving along a line of constant flame angle.

Future work will focus on establishing a relationship between the stability characteristics and flame structure results presented in this paper in order to obtain an improved understanding of the phenomenology of unstable combustion.

## References

- [1] T. Poinso, A. Trounev, D. Veynante, S. Candel, E. Sspositi, "Vortex-Driven Acoustically Coupled Combustion Instabilities," *J. Fluid Mech.*, Vol. 177, 1987, pp.265-292.
- [2] K.C. Schadow, E. Gutmark, T.P. Parr, D.M. Parr, K.J. Wilson and J.E. Crump, "Large-Scale Coherent Structures as Drivers of Combustion Instability," *Combustion Science & Technology*,



- Vol. 64, 1989, pp. 167-186.
- [3] K.K. Venkataraman, L.H. Preston, D.W. Simons, B.J. Lee, J.G. Lee and D.A. Santavicca, "Mechanism of Combustion Instability in a Lean Premixed Dump Combustor," *Journal of Propulsion and Power*, Vol.15, No. 6, 1999, pp. 909-918.
- [4] D. Straub, G. Richards, M.J. Yip, W.A. Rogers and E.H. Robey, "Importance of Axial Swirl Vane Location on Combustion Dynamics For Lean Premix Fuel Injectors," 34th AIAA/ASME/SAE/ASEE Joint Propulsion Conference and Exhibit, AIAA 98-3909, July 1998.
- [5] T. Lieuwen and B.T. Zinn, "A Mechanism of Combustion Instability in Lean Premixed Gas Turbine Combustors," *International Gas Turbine & Aeroengine Congress & Exhibition*, 99-GT-003, 1999.
- [6] J.G. Lee, K. Kim and D.A. Santavicca, "Measurement of Equivalence Ratio Fluctuation and Its Effect in Heat Release During Unstable Combustion," *Proceedings of the Combustion Institute*, Volume 28, 2000, pp. 415-421.
- [7] S. Sivasegaram and J.H. Whitelaw, "Oscillations in Axisymmetric Dump Combustors," *Combustion Science & Technology*, Vol. 52, 1987, pp. 413-426.
- [8] W-P Shih, J.G. Lee and D.A. Santavicca, "Stability and Emissions Characteristics of a Lean Premixed Gas Turbine Combustor," *Proceedings of the Combustion Institute*, Volume 26, 1996.
- [9] D. L. Straub and G. A. Richards, "Effects of Fuel Nozzle Configuration on Premix Combustion Dynamics," *International Gas Turbine & Aeroengine Congress & Exhibition*, 98-GT-492, 1998.
- [10] G.A. Richards and M.C. Janus, "Characterization of Oscillations During Premix Gas Turbine Combustion", *Journal of Engineering for Gas Turbine and Power*, Vol. 120, 1998, pp. 294-301.
- [11] A. A. Peracchio and W. M. Proscia, "Nonlinear Heat-Release/Acoustic Model for Thermoacoustic Instability in Lean Premixed Combustors," *International Gas Turbine & Aeroengine Congress & Exhibition*, 98-GT-269, 1998.
- [12] J. M. Cohen, B.E. Wake and D. Choi, "An Investigation of Instabilities in a Lean, Premixed Step Combustor", *Journal of Propulsion and Power*, Vol. 19, 2003, pp. 81-88.
- [13] J.G. Lee, K. Kim and D.A. Santavicca, "A Study of the Role of Equivalence Ratio Fluctuations During Unstable Combustion in a Lean Premixed Gas Turbine Combustor", 38th AIAA/ASME/SAE/ASEE Joint Propulsion Conference and Exhibit, AIAA Paper 2002-4015, July 2002.
- [14] A. Lozano, "Laser-excited Luminescent Tracers for Planar Concentration Measurements in Gaseous Jets," High Temperature Gasdynamics Laboratory, Stanford University, HTGL Rept. T-284, Aug. 1992.
- [15] C. J. Dasch, "One-Dimensional Tomography: a Comparison of Abel, Onion-Peeling, and Filtered Backprojection Methods," *Applied Optics*, Vol. 31, 1992, pp. 1146-1152.